ANNALS of Clinical and Translational Neurology
Open Access
AMERICAN NEUROLOGICAL ASSOCIATION

RESEARCH ARTICLE

Identification and functional characterization of novel *GDAP1* variants in Chinese patients with Charcot–Marie–Tooth disease

Cong-Xin Chen[1,2,a], Jia-Qi Li[1,a], Hai-Lin Dong[1], Gong-Lu Liu[1], Ge Bai[3] & Zhi-Ying Wu[1]

[1]Department of Neurology and Research Center of Neurology in Second Affiliated Hospital, and Key Laboratory of Medical Neurobiology of Zhejiang Province, Zhejiang University School of Medicine, Hangzhou, China
[2]Department of Neurology and Institute of Neurology, First Affiliated Hospital, Fujian Medical University, Fuzhou, China
[3]NHC and CAMS Key Laboratory of Medical Neurobiology, MOE Frontier Science Center for Brain Research and Brain-Machine Integration, School of Brain Science and Brain Medicine, Zhejiang University, Hangzhou, China

Correspondence
Zhi-Ying Wu, Department of Neurology and Research Center of Neurology in Second Affiliated Hospital, and the Collaborative Innovation Center for Brain Science, Zhejiang University School of Medicine, 88 Jiefang Road, Hangzhou 310009, China. E-mail: zhiyingwu@zju.edu.cn

Funding Information
This work was supported by grants from the National Natural Science Foundation of China (81125009, 31871022), the Fundamental Research Funds for the Central Universities (2019XZZX001-01-04), and the research foundation for the distinguished scholar of Zhejiang University to Zhi-Ying Wu (188020-193810101/089).

Received: 22 July 2020; Revised: 14 September 2020; Accepted: 1 October 2020

Annals of Clinical and Translational Neurology **2020; 7(12): 2381–2392**

doi: 10.1002/acn3.51233

[a]The first two authors contributed equally to this work.

This manuscript was uploaded to a preprint server (https://doi.org/10.22541/au.159110407.77885838).

Abstract

Objective: To identify and characterize the pathogenicity of novel variants in Chinese patients with Charcot–Marie–Tooth disease. **Methods**: Multiplex ligation-dependent probe amplification (MLPA) and whole-exome sequencing (WES) were performed in 30 unrelated CMT patients. Minigene assay was used to verify the effect of a novel splicing variant (c.694+1G>A) on pre-mRNA. Primary fibroblast cell lines were established from skin biopsies to characterize the biological effects of the novel variants p.L26R and p.S169fs. The mitochondrial structure was observed by an electron microscope. The expression level of protein was analyzed by Western Blotting. Mitochondrial dynamics and mitochondrial membrane potential (MMP, $\Delta\psi m$) were analyzed via immunofluorescence study. Mitochondrial ATP levels were analyzed via bioluminescence assay. The rate of oxygen consumption was measured with a Seahorse Bioscience XF-96 extracellular flux analyzer. **Results**: We identified 10 pathogenic variants in three known CMT related genes, including three novel variants (p.L26R, p.S169fs, c.694+1G>A) and one known pathogenic variant (p.R120W) in *GDAP1*. Further, we described the clinical features of patients carrying pathogenic variants in *GDAP1* and found that almost all Chinese CMT patients with *GDAP1* variants present axonal type. The effect of c.694+1G>A on pre-mRNA was verified via minigene splice assay. Cellular biological effects showed ultrastructure damage of mitochondrial, reduced protein levels, different patterns of mitochondrial dynamics, decreased mitochondrial membrane potential ($\Delta\psi m$), ATP content, and defects in respiratory capacity in the patient carrying p.L26R and p.S169fs in *GDAP1*. **Interpretation**: Our results broaden the genetic spectrum of *GDAP1* and provided functional evidence for mitochondrial pathways in the pathogenesis of *GDAP1* variants.

Introduction

Charcot–Marie–Tooth (CMT) disease refers to a group of inherited sensorimotor peripheral neuropathies with an estimated incidence of 4 in 10 000 individuals. CMT has been traditionally subdivided into demyelinating type (CMT1) and axonal type (CMT2) based on the electrophysiological results.[1] CMT caused by mutations in the ganglioside-induced differentiation-associated protein 1 (*GDAP1*) gene is clinically characterized by a severe distal motor and sensory neuropathy. But a broad spectrum of phenotypes should be considered because of the

variability in different inheritance patterns.[2,3] Phenotype-genotype correlations for mutations have been rarely investigated in the Asian area besides few cases reported.[4-9] The locus of chromosome 8q13.q21 was first identified to be linked to recessive CMT cases in Tunisian families.[10] Then the corresponding gene, *GDAP1*, was found in 2002 by Baxter et al.[11] Unlike many other CMT disease-causing genes, it is associated with an axonal (CMT2K; MIM# 607831), a demyelinating (CMT4A; MIM# 214400), and an intermediate form (CMTRIA; MIM# 608340) of CMT with recessive or dominant modes of inheritance.[12] It is now clear that the different modes of inheritance of CMT caused by mutations in *GDAP1* show distinct clinical and electrophysiological features. In the autosomal recessive form, patients usually have more severe clinical characteristics such as early onset and disabilities due to wasting. However, it is common for patients with autosomal dominant trait to be associated with late-onset and rather mild phenotype.[13]

GDAP1 gene encodes a 358-amino acid protein. As an integral membrane protein of the external mitochondrial membrane, it is mainly expressed in neurons.[14,15] However, the explicit molecular mechanism underlying the *GDAP1* function remains unclear. Available data indicate an important role of *GDAP1* in many aspects of mitochondrial morphology and functioning such as mitochondrial dynamics,[14-17] formation and/or modulation of the ER-mitochondria contacts,[18] and mitochondrial transport.[18,19] A recent study showed that neuroinflammation was also involved in the pathophysiology of axonal GDAP1-related CMT.[20] To sum up, the present research demonstrates that mutations in the *GDAP1* gene cause a loss-of-function process of the mutant proteins. Dysfunction of the GDAP1 protein may lead to overall mitochondrial impairment including many pathological events. All the defects may contribute to the symptoms of the disease and modulate the severity and course of the symptoms.

Herein, we provide the clinical features, frequency of distribution, and physiopathology of patients with novel *GDAP1* variants in a cohort of southeast Chinese patients with CMT by performing multiplex ligation-dependent probe amplification (MLPA) and whole-exome sequencing (WES). Then the variants were further characterized by functional studies.

Materials and methods

Subjects

Thirty unrelated patients clinically diagnosed with CMT were enrolled consecutively between September 2018 and August 2019 from southeastern China. Clinical evaluations and neurological examinations were performed by at least two senior neurologists. Five hundred unrelated phenotypically normal controls with no known family history of CMT were included in the study. Written informed consent was obtained from all the subjects or their guardians. This study was approved by the ethics board of Second Affiliated Hospital, Zhejiang University School of Medicine.

DNA extraction and whole-exome sequencing

Genomic DNA samples were extracted from peripheral blood lymphocytes using a DNA isolation kit (Qiagen, Germany). WES was performed using the Agilent SureSelect Human All Exome V6 kit (Agilent Technologies Inc, Canada) on an Illumina HiSeq X Analyzer (Illumina, USA) with 150-bp paired-end runs. SIFT (http://sift.jcvi.org/), PolyPhen-2 (http://genetics.bwh.harvard.edu/pph2/), and MutationTaster (http://www.mutationtaster.org/) were used to predict the possible protein functional change caused by a variant. The frequency in the general population of the identified variants was checked using the Single-Nucleotide Polymorphism (dbSNP) Database (https://www.ncbi.nlm.nih.gov/snp/), Exome Aggregation Consortium (ExAC) database (http://exac.broadinstitute.org/), the 1000 Genomes Project (https://www.ncbi.nlm.nih.gov/variation/tools/1000 genomes/), and The Genome Aggregation Database (http://gnomad-old.broadinstitute.org/). All the potential variants were validated by Sanger sequencing.

Minigene assay

Exonic and at least 150 bp of flanking 5′ and 3′ intronic *GDAP1* sequences (RefSeq NM_018972) from genomic DNA of proband of family 1 and control were PCR-amplified using KOD-Plus-Neo DNA Polymerase (TOYOBO, Japan), with primers carrying restriction sites for XhoI and EcoRI (5′-GGTACGGGATC ACCAGAATTCTC-CACTCGCCGTTTAACTC-3′ (forward) and 5′-ATCCTG-CAG CGGCCGCTCGAGCCCACGTGCTGGTCCTTATT-3′ (reverse). PCR products were subcloned into the splicing reporter pSPL3 vector using T4 DNA Ligase (New England Biolabs, USA). The pSPL3 vector contains a minigene. Transcription occurs from the SV40 promoter and the RNA undergoes splicing under the control of the host cell's RNA splicing machinery, resulting in the fusion of two vector exon sequences. If a genomic DNA fragment cloned into pSPL3 contains an exon with functional splice donor (SD) and splice acceptor (SA) sequences, a different splicing pattern (the complete skipping of genomic DNA fragment) may occur. Minigene constructions were confirmed by Sanger sequencing. For minigene

assay, HEK293T cells were maintained at 37°C/5%CO_2 in Dulbecco's modified Eagle's medium (DMEM) (GIBCO, USA) supplemented with 10% fetal bovine serum (FBS) (GIBCO, USA), 100 IU/mL of penicillin and 100 μg/mL of streptomycin (HyClone, USA). Cells were transfected with expression vectors using Lipofectamine 3000 (Invitrogen, USA) according to the manufacturer's instructions. After 36 h, total RNA was extracted by RNAiso Plus (Takara, Japan) and then was reverse transcribed into cDNA using the PrimeScript RT reagent Kit (Takara, Japan), following the manufacturer's protocol. Finally, PCR products were visualized in 10% agarose gels to study the transcript band pattern and then identify potential changes in the splicing process by Sanger sequencing.

Primary fibroblasts culture and treatment

Primary fibroblast cell lines were established from skin biopsies with punches (Electron microscopy sciences, USA), acquired from the proband of family 2. Written consent was obtained from the guardians of this patient. Fibroblasts were maintained in DMEM (GIBCO, USA) with low glucose (1g/L) and sodium pyruvate supplemented with 10% FBS (GIBCO, USA).

Transmission Electron microscopy

Muscular biopsy was performed in the proband of family 2 to observe the ultrastructure of mitochondria in muscular tissue. Muscular tissue was fixed in 2.5% glutaraldehyde (Sangon Biotech, China) in PBS at 4°C for 2 h. Then, the tissue block was washed three times with PBS, and the block embedded with agar were fixed again with 1% osmium tetroxide for 2 h then washed three times with PBS. The tissue block was dehydrated with an ethanol series and fixed again with Epon 812 (Sangon Biotech, China). The ultrathin (70 nm) sections were collected on Formvar/carbon-coated nickel grids (Sangon Biotech, China), and the grids were stained with 2.5% uranyl acetate (Sangon Biotech, China) for 7 min followed by lead citrate (Sangon Biotech, China) for 2.5 min, and then the sections were observed with a JEM-1011 electron microscope (JEOL, Japan).

Western blotting

The cells were harvested in the cell lysis reagent (Sigma, USA) supplemented with a 1% protease inhibitor PMSF (Beyotime, China) and centrifuged at 13,000 rpm for 20 min at 4°C. Western blot was performed as previously described.[21] Protein extracts were separated on 10% SDS-PAGE gels and immunoblotted with primary antibodies (Abnova, Taiwan, China). HRP-conjugated secondary antibodies (Santa Cruz, USA) were used to detect primary antibodies. The densitometric values of the bands of three independent experiments were analyzed using Adobe Photoshop software and were normalized to β-Tubulin levels.

Confocal microscopy

Primary fibroblasts were grown in 35-mm glass bottom dishes (Sangon Biotech, China). Cells were incubated with MitoTracker® Red (Invitrogen, USA) and DAPI Reagent (Sigma, USA) and then were directly observed under a confocal microscope (Leica, Germany).

Analysis of mitochondrial membrane potential (MMP, $\Delta\psi m$)

Mitochondrial membrane potential was determined using tetramethylrhodamine methyl ester perchlorate, TMRM (Invitrogen, USA). Cells were fixed and stained according to the manufacture's recommended protocol. An Olympus microscope equipped with a CCD camera was used for the acquisition of fluorescent images. The average fluorescent intensities were quantified using ImagePro Plus version 5.0 imaging software.

Measurement of ATP content

ATP content was determined in fibroblasts lysates using an ATP bioluminescence assay kit (Perkin Elmer, USA), according to the manufacture's recommended protocol. Measurements were performed in a luminometer (Perkin Elmer, USA).

Measurement of oxygen consumption

The rate of oxygen consumption in fibroblasts was measured with a Seahorse Bioscience XF-96 extracellular flux analyzer (Seahorse Bioscience, USA). XF96 creates a transient 7μl-chamber in specialized microplates that allows for the determination of oxygen and proton concentrations in real-time. To allow comparison between different experiments, data are expressed as the rate of oxygen consumption in pmol/min and the rate of extracellular acidification in mpH/min, normalized to cell protein in individual wells determined by the Bradford protein assay (Bio-Rad, USA). A density of 20000 cells per well in a 96-well plate was coated with Cell-Tak^{TM} adhesive. The rate of O2 was determined under basal condition and the addition of oligomycin (1.5μM), carbonyl cyanide *p*-(trifluoromethoxy) phenylhydrazone (FCCP) (0.5μM), rotenone (1μM), and antimycin A (1μM).

Statistical analysis

All the values are expressed as the mean ± SD, and the data were analyzed by one-way ANOVA or two-way ANOVA using GraphPad Prism software. P values less than 0.05 were considered statistically significant.

Results

Genetic analysis

MLPA and WES were performed on 30 unrelated CMT patients. Eight patients had *PMP22* duplication. Ten variants in three known genes related to CMT, including three novel variants (p.L26R, p.S169fs, c.694 + 1G>A) and one known variant (p.R120W) in *GDAP1* gene (Figure 1A, B) and six known pathogenic variants of other genes (p.R280H and p.R259L in *MFN2*; p.V181M, c.-103C> T, p.V91M and p.R183H in *GJB1*) (Figure S1), were identified in nine index patients. No variant was detected in the remaining 13 cases. The three novel variants were absent or with low frequency in several global human genome databases such as 1000G and ExAC. After assessing by SIFT, PolyPhen-2 software, and MutationTaster, all of them were predicted to cause deleterious disruptions to the protein. According to the American College of Medical Genetics and Genomics (ACMG) standards and guidelines, two were assigned as "pathogenic variants" and one as "likely pathogenic variant" (Table 1).

Besides the three families carrying variants in *GDAP1* in this study, we have previously reported three *GDAP1* variants (p.W31*, p.Q38*, p.V215I) in two patients[22]. The locations of seven variants from our studies and 10 variants from other Chinese studies in the structure of *GDAP1* protein are shown in Figure 1C. Taking all the probands in our studies into consideration, we can summarize a frequency of 2.78% (5/180) in *GDAP1* in our CMT patients.

Clinical features of patients with *GDAP1* variants

Three novel and one known pathogenic variants in the *GDAP1* gene were identified in three families affected with axonal type CMT (Figure 1A). In family 1, the proband with a homozygous splicing variant c.694 + 1G>A was a 30-year-old man without a family history of consanguinity. The onset of the disease was at age 5. He could not walk alone until he was 3 years old. He had difficulty in walking and hand manipulation and received three times surgery of deformity correction due to the severe foot deformity. The patient complained about obvious weakness and muscle atrophy in all the limbs. Additionally, he had a sensory loss and depressed deep tendon reflexes. The other affected individuals in this family included the proband's younger brother and cousin showed similar symptoms and electrophysiological properties. They carried the same variant and had foot deformities and progressive distal muscle weakness and atrophy in all the limbs. The electrophysiological study showed severe damage to axon.

In family 2, the proband carrying p.L26R and p.S169fs was a 5-year-old boy with a history of unsteady gait and foot drop for a year. The disease presented slowly progressive. He could not walk alone until he was 2 years old. Symptoms of foot drop began from right to left. The distal muscle atrophy began in his feet, followed by leg muscle involvement. He had a severe foot deformity and received surgery of deformity correction at the age of 5. Neurological examinations showed distal muscle weakness and atrophy in lower limbs, without impairment of proximal muscles. All deep tendon reflexes were weakened.

The proband of family 3 harbored a known heterozygous missense mutations p.R120W. She was a 73-year-old female with normal motor milestones who had a history of distal weakness and sensory loss in the lower limbs for over 10 years. Gradually, she had difficulty in walking and climbing stairs. She could get around only using a crutch since the age of 72. No family history was identified. Her daughter carried the same variant has no symptoms at all. The detailed clinical features of patients carrying *GDAP1* pathogenic variants are shown in Table 2.

Splicing assays of novel variant c.694 + 1G>A in *GDAP1*

To validate the functional classification of the novel splicing variant c.694 + 1G>A identified in family 1, minigene splice assay was conducted. Exon 5 (115bp) and 150bp of flanking 5′ and 3′ intronic sequences in the *GDAP1* gene from genomic DNA of proband of family 1 and control

Figure 1. *GDAP1* variants identified in patients with CMT2K. (A) Pedigrees of three CMT families carried *GDAP1* variants. Arrows indicate the proband of each family. (B) Sequence chromatograms of four variants in *GDAP1* are shown. The lower chromatogram in each frame represents the variant, while the upper one represents the normal sequence. (C) Domain structure of *GDAP1* protein and the location of variants in the *GDAP1* protein in Chinese patients. *GDAP1* contains two typical glutathione-S transferases (GST-N and GST-C). A single-transmembrane domain (TMD) at the extremity of the C-terminal. A hydrophobic domain (HD) in the flanking C terminal region and two additional regions constituting the α4–α5 loop. Novel variants identified in our team are in orange and known variants are in red. Other reported variants in other Chinese studies are in black.

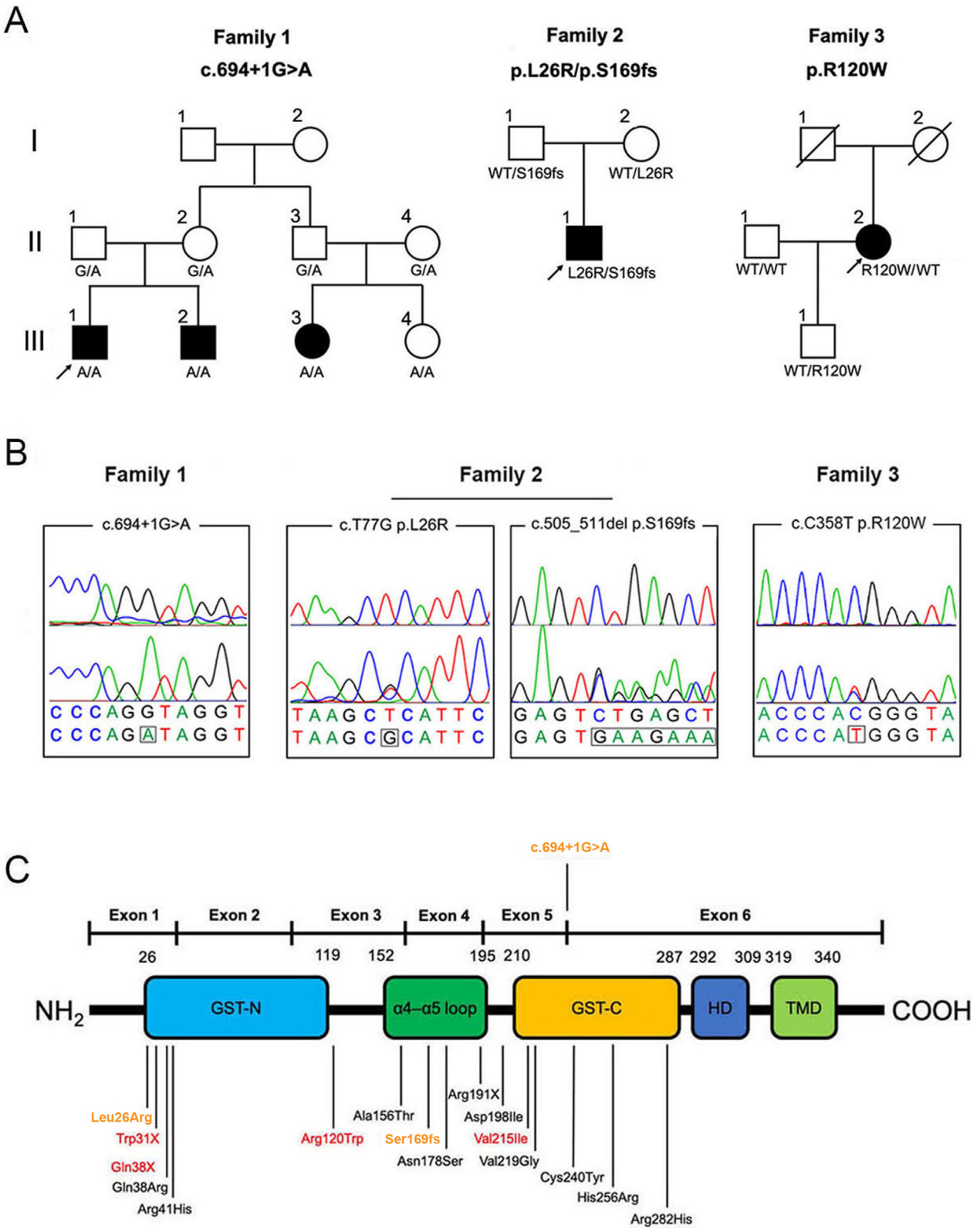

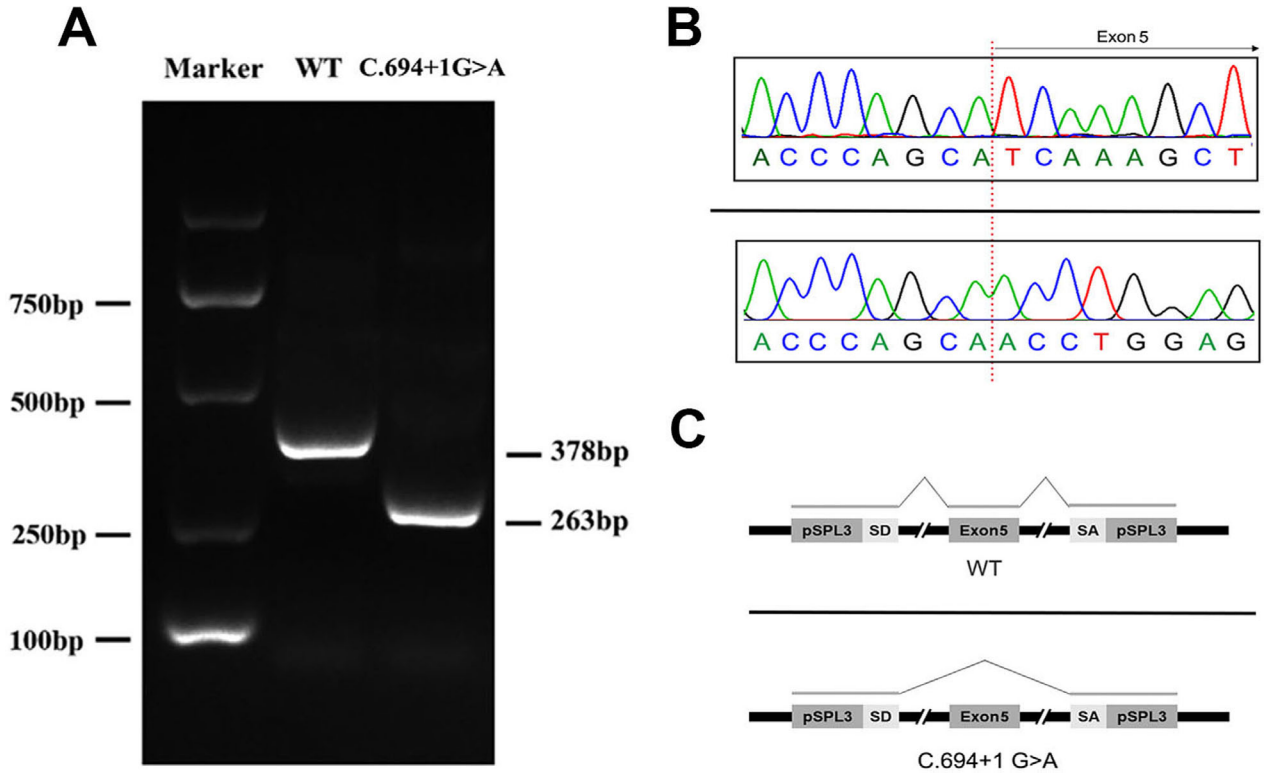

Figure 2. Splicing alteration was identified by a minigene assay. (A) cDNA products were separated by agarose gel electrophoresis. Lane1: Marker; Lane2: WT [263 bp + 115bp (exon 5)]; Lane3: c.694 + 1G>A variant 263 bp. (B) The sequencing results for the bands. (C) Schematic diagram of minigene construction. Splice donor (SD) and splice acceptor (SA) are two exons of the pSPL3 vector.

were subcloned into the pSPL3 vector. Mutant and control minigene were transfected into HEK293 T cells. RNA was extracted and reverse-transcribed into cDNA after plasmid transfection of cells for 48 h. Agarose gel electrophoresis showed a mutant band that is smaller than the WT band (Figure 2A). Sequencing analysis showed a loss of Exon 5 (115bp) in mutant minigene (Figure 2B). The schematic diagram of the affected splicing products is shown in Figure 2C. These results verified the effect of the c.694 + 1G>A in *GDAP1* on pre-mRNA.

Functional analyses of novel variants p.L26R and p.S169fs in *GDAP1*

To elucidate the biological effects of the novel variants p.L26R and p.S169fs identified in family 2, we studied their function in muscle tissue and fibroblasts from the proband of family 2. Transmission electron microscopy was used to observe the ultrastructure in the muscle tissue of patient. In Figure 3, obvious damage of mitochondrial structure including the disorganization of cristae and disruption of the mitochondrial membrane was found in muscle tissue of the patient carrying p.L26R and p.S169fs variants. We further analyzed the expression level of mutant *GDAP1*. Western blot results revealed that mutant protein in muscle tissue of the patient was markedly reduced compared to that of WT *GDAP1* (Figure 4A, B). Actually, mutant protein in patient-derived fibroblasts also showed an undetectable band compared to that of WT *GDAP1* (Figure S2A, B 2A, B).

To evaluate the mitochondrial distribution pattern, mitochondria were visualized using MitoTracker Red staining. We found the mitochondrial network was more fragmented and contained a larger number of short mitochondria in patient-derived fibroblasts than control fibroblasts (Figure 4C,D). Additionally, tetramethylrhodamine methyl ester perchlorate (TMRM) was used to validate the level of mitochondrial membrane potential (MMP, $\Delta\psi m$). $\Delta\psi m$ is shown in red represented by the relative intensity of the TMRM signal. We found the optical intensity was reduced by 26.2% in patient-derived fibroblasts compared with control 1 ($n = 3$, $P = 0.0048$), and 23.9% compared with control 2 ($n = 3$, $P = 0.0035$) (Figure 4E, F). To further determine whether intracellular reactive oxygen species (ROS) showed increased production due to the loss of $\Delta\psi m$, MitoSOX Red, a fluorogenic dye for the selective detection of superoxide in the mitochondria of live cells was used. The result showed that no

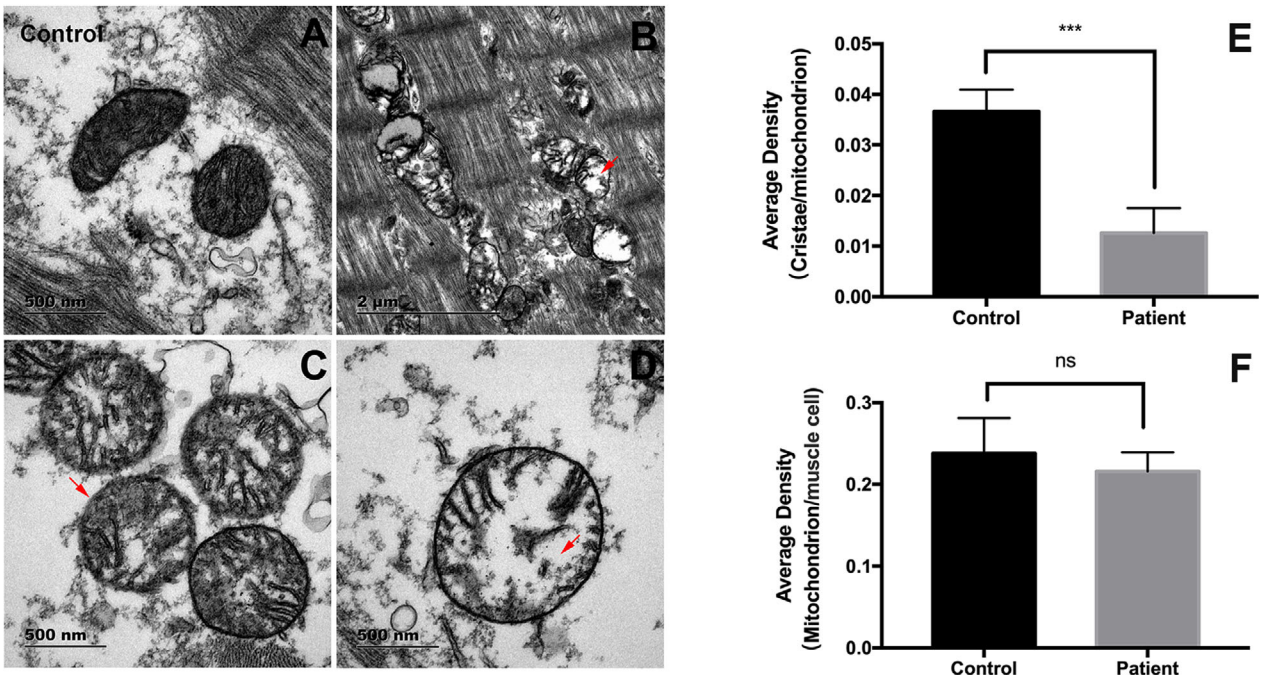

Figure 3. Transmission electron microscopic analysis of mitochondrial structure in muscle tissue. (A) The mitochondrial structure of the control subject. (B-D) Compared with the control, *GDAP1* mutations resulted in damage to mitochondria, including disruption of the mitochondrial membrane (C) and disorganization of cristae (B, D) (red arrows). (E) Quantitation of the number of cristae per mitochondria. (F) The mitochondrial density per cell.

significant changes in the ROS level between patient-derived fibroblasts and control fibroblasts (Figure S2C).

The capacity of oxidative phosphorylation in mutant and control fibroblasts was examined by measuring the levels of cellular and mitochondrial ATP using a luciferin/luciferase assay. Fibroblasts were incubated in the media in the presence of glucose, and 2-deoxy-d-glucose with pyruvate. As shown in Figure 4G, the levels of ATP production in mutant fibroblast in the presence of glucose (total cellular levels of ATP) decreased by 44.6% compared with those measured in the control fibroblast ($n = 5$, $P < 0.0001$). In Figure 4H, the levels of ATP production in mutant fibroblasts in the presence of pyruvate and 2-deoxy-d-glucose which can inhibit glycolysis (mitochondrial levels of ATP) decreased by 40.3% relative to control fibroblasts ($n = 5$, $P < 0.0001$). ATP bioluminometers analysis revealed that the relative ATP production was apparently decreased in the patient-derived fibroblasts.

To further evaluate alterant cellular bioenergetics in mutant fibroblasts, we examined the oxygen consumption rates (OCR) of it and control fibroblasts. As shown in Figure 4I and Figure 4J, the basal OCR in the mutant cell lines decreased by 13.2% ($n = 3$, $P = 0.0056$) relative to the control fibroblasts. OCR were measured after the sequential addition of oligomycin (to inhibit the ATP synthase), FCCP (to uncouple the mitochondrial inner membrane and allow for maximum electron flux through the ETC), rotenone (to inhibit complex I), and antimycin A (to inhibit complex III). The ATP-linked OCR, maximal OCR and reserve capacity in mutant fibroblasts decreased by 16.5%, 15.1%, 15.3% ($n = 3$, $P = 0.0113$, 0.0114, 0.0335) relative to the control fibroblasts, respectively. However, proton leak OCR and non-mitochondrial OCR showed no significance between mutant and control fibroblasts.

Discussion

In this study, we applied MLPA and WES in 30 unrelated clinically diagnosed CMT patients from southeast China. Finally, 17 out of 30 patients were genetically diagnosed with CMT, including eight patients with *PMP22* duplication, four with known *GJB1* variants, three with *GDAP1* variants (three novel and one known), and two with known *MFN2* variants. Herein, we focus on the three novel variants (p.L26R, p.S169fs, c.694 + 1G>A) and one known variant (p.R120W) in *GDAP1*. Taking three variants previously reported in two patients into consideration,[22] we can summarize a frequency distribution of 2.78% (5/180) in *GDAP1*. Previous studies in the Chinese population showed a similar frequency.[4,9] In studies

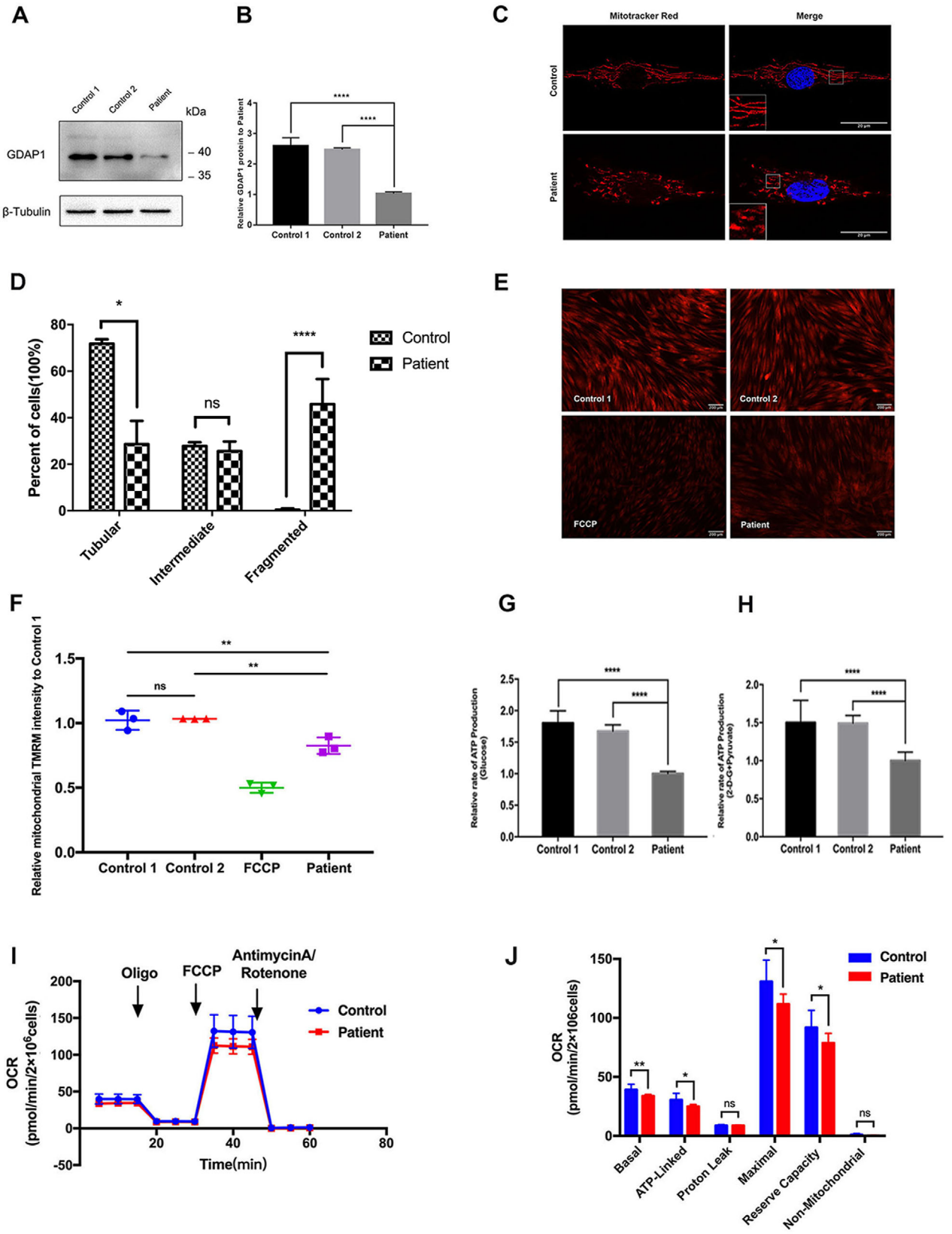

Figure 4. Function studies of mutant *GDAP1* and control in muscle tissue and patient-derived fibroblasts. (A) Western blot analysis of protein extracts obtained from muscle tissue of proband 2. The anti-GDAP1 antibody was used to detect the protein. (B) Values represent mean ± SD (n = 3, ****P < 0.0001). (C) Staining of mitochondria marker (MitoTracker, red) and DAPI (blue) in fibroblasts from the Control (upper panel) and the patient (lower panel). Insets in the images are enlarged (original magnification, ×4.0) to the left bottom. Scale bar, 20 μm. (D) Quantification of cells with different mitochondrial morphologies to total cell (n = 3, ****P < 0.0001). (E) TMRM staining was used to measure MMP ($\Delta\psi m$) in fibroblasts from the Control (upper panel) and the patient (bottom right panel). FCCP was used as the positive control. Scale bar, 200 μm. (F) Statistical analysis of D (n = 3, **P < 0.01). (G) Measurement of cellular ATP levels using bioluminescence assay. Fibroblast was incubated with 10 mmol/L glucose and ATP bioluminometers analysis revealed a significant decrease of ATP content in the patient-derived fibroblast (n = 5, ****P < 0.0001). (H) Measurement of mitochondrial ATP levels using bioluminescence assay. Fibroblast was incubated with 5 mmol/L 2-deoxy-D-glucose plus 5 mmol/L pyruvate which can inhibit glycolysis. The result revealed a significant decrease in the ATP content in the patient-derived fibroblast (n = 5, ****P < 0.0001). (I) An analysis of O2 consumption in the mutant and control fibroblast using different inhibitors. The rates of O2 (OCR) were first measured on 2×10^4 cells under basal condition and then sequentially added to oligomycin (1.5 μmol/L), carbonyl cyanide p-(trifluoromethoxy) phenylhydrazone (FCCP) (0.5 μmol/L), rotenone (1μmol/L), and antimycin A (1 μmol/L) at indicated times to determine different parameters of mitochondrial functions. (J) Graphs presented the ATP-linked OCR, proton leak OCR, maximal OCR, reserve capacity, and non-mitochondrial OCR in mutant and control fibroblast. Non-mitochondrial OCR was determined as the OCR after rotenone/antimycin A treatment. Basal OCR was determined as OCR before oligomycin minus OCR after rotenone/antimycin A. ATP-linked OCR was determined as OCR before oligomycin minus OCR after oligomycin. Proton leak was determined as basal OCR minus ATP-linked OCR. Maximal was determined as the OCR after FCCP minus non-mitochondrial OCR. Reserve capacity was defined as the difference between maximal OCR after FCCP minus basal OCR. The average of four determinations for each fibroblast is shown.

Table 1. Three novel variants in *GDAP1* genes identified in our study

Nucleotide change	Amino acid change	1000G	ExAC	SIFT	Polyphen-2 (HDIV)	MutationTaster	ACMG
c.T77G (Het)	p.L26R	0	0.000008267	Deleterious	Probably damaging	Disease causing	Likely Pathogenic (PM1+PM2+PM3+PP1)
c.505_511del (Het)	p.S169fs	0	0	-	-	Disease causing	Pathogenic (PVS1+PM1+PM2+PP1+PP3)
c.694+1G>A (Hom)	-	0	0	-	-	Disease causing	Pathogenic (PVS1+PM2+PP1)

ACMG, the American College of Medical Genetics and Genomics; ExAC, Exome Aggregation Consortium; Het, heterozygotes; Hom, homozygotes; 1000G, 1000 Genomes Project.

conducted in other Asian CMT patients, the frequency of *GDAP1* mutation ranged from 1 to 2.8%,[6,8,23] which was generally lower than those reported in the Mediterranean region (5.4%–11.5%).[24-28]

It is noticeable, however, all the patients with *GDAP1* variants in our study presented the axonal type of neuropathy which was consistent with previous studies in Chinese patients except one of the patients reported by He J.[29] Actually, this case showed an absent MNCV and CMAPs in the median nerve as no response by electrophysiological detection. As a result, it caused difficulty in defining the patient's clinical type of CMT. And a study conducted in a cohort of 1,030 patients with inherited peripheral neuropathies in Japan showed all 10 patients with *GDAP1* mutations indicated axonal type peripheral neuropathy. However, patients presented demyelinating type were more common in European and Mediterranean region.[11,30-33]

To further characterize the pathogenicity of these novel variants, the functional study was applied to verify the effect of the novel splicing variant (c.694+1G>A) on pre-mRNA and the biological effects of two novel variants (p.L26R and p.S169fs). It is well known that *GDAP1*, located in the external mitochondrial membrane, is mainly expressed in neurons, and is involved in many aspects of mitochondrial morphology and functioning.[14,15] Impairment of mitochondrial function can cause a reduced mitochondrial membrane potential, ATP production, and unbalanced mitochondrial dynamics. *GDAP1* regulates mitochondrial dynamics which was confirmed in a number of studies.[14,16,34] *GDAP1* may interact with transport protein involved in mitochondrial transport and movement,[19] and impaired transport of mitochondria may offer a potent mechanism that may account for axonal loss in CMT patients with *GDAP1* mutations. Recent findings have revealed that *GDAP1* is also associated with

Table 2. Clinical features of patients carrying *GDAP1* variants.

Family	Variants	Inheritance pattern	Sex	AAO, y	Symptoms at onset	Sensory loss	Skeletal deformities	Muscle weakness	Muscle atrophy	Median nerve, MNCV, m/s CMAP, mV	Tibial nerve, MNCV, m/s CMAP, mV	Median nerve, SNAP, uV
Family 1	c.694 + 1G>A	AR	Male	5	distal weakness and atrophy	Yes	Pes cavus	UL + LL	UL + LL	NA;NA	45.3;2.8	0.6
Family 2	c.T77G; p.L26R c.505_511del; p.S169fs	Sporadic	Male	4	Gait disturbance and distal weakness	No	Pes cavus	UL + LL	LL	52.7;1.3	NA;0.2	3.8
Family 3	c.358C> T; p.R120W	Sporadic	Female	63	weakness of lower limbs	Yes	Pes cavus	LL	NA	NA;NA	38.9;0.07	1.32

AAO, age at onset; CMAP, compound muscle action potential of the median nerve; LL, lower limbs; MNCV, motor nerve conduction velocity; SNAP, sensory nerve action potential; UL, upper limbs.

mitochondria-associated membranes (MAMs), and altered *GDAP1* level may affect the formation or functioning of the ER-mitochondria contacts[18] which could further disrupt calcium homeostasis, mitochondrial dynamics, and transport of mitochondria. In the present study, fibroblasts from autosomal-recessive CMT2K patients showed reduced *GDAP1* expression levels, fragmentation of the mitochondrial, a declining mitochondrial membrane potential, respiration defects, and decreased cellular and mitochondrial ATP production which indicates loss of *GDAP1* protein cause impairment of mitochondrial function. Those changes were mostly confirmed by the previous studies.[14,16,34-36] The p.S169fs led to the appearance of the premature stop codon. It could result in the rapid degradation of *GDAP1* protein and cause severe phenotype with disease onset in the first decade.[12,14] The p.L26R lies in GST domains, which function as a redox sensor, rather than an authentic GST enzyme.[37] It may modulate its function by changing its conformational state upon stimulation and *GDAP1* expression may be protective by its GST activity.[37] Therefore, we speculate that the p.L26R may further reduce *GDAP1* protein which has had an amplified effect on pathologic changes. Decreased MMP ($\Delta\psi m$) and mitochondrial ATP production indicated cellular injury and actually can also trigger the fragmentation of mitochondria.[38] The OCR assay showed respiratory deficiency in mutant fibroblasts could also result in decreased efficiency of the mitochondrial ATP synthesis. In addition, transmission electron microscopy showed a distinct disruption of the mitochondrial membrane and disorganization of cristae in muscular tissue. There are no studies about the changes in mitochondria in CMT patients caused by *GDAP1* mutations under the transmission electron microscope. Those findings indicated its role in possibly impair cellular energetics, and consequently, in cellular function.[39] To sum up, all these results show that the mitochondrial-mediated pathway plays a key role in the pathogenesis of *GDAP1* and can ultimately be characterized as the pathogenicity of these two variants.

In conclusion, we identified and classified the pathogenicity of three novel *GDAP1* variants, which broaden the genetic spectrum of *GDAP1*. Further, we described the clinical features of CMT patients carrying pathogenic variants in *GDAP1* and found that almost all Chinese CMT patients with *GDAP1* variants present axonal type. Additionally, we identified the ultrastructure damage of mitochondrial and emphasized the function of GDAP1 in the mitochondrial-mediated pathway.

Acknowledgments

The authors sincerely thank the participants for their help and willingness to participate in this study. This work

was supported by grants from the National Natural Science Foundation of China (81125009, 31871022), the Fundamental Research Funds for the Central Universities (2019XZZX001-01-04), and the research foundation for the distinguished scholar of Zhejiang University to Zhi-Ying Wu (188020-193810101/089).

Conflict of Interest

All authors declare no conflicts of interest.

References

1. Pareyson D, Marchesi C. Diagnosis, natural history, and management of Charcot-Marie-tooth disease. Lancet Neurol. 2009;8:654–667.
2. Azzedine H, Ruberg M, Ente D, et al. Variability of disease progression in a family with autosomal recessive CMT associated with a S194X and new R310Q mutation in the GDAP1 gene. Neuromuscul Disord 2003;13:341–346.
3. Manganelli F, Pisciotta C, Nolano M, et al. A novel autosomal dominant GDAP1 mutation in an Italian CMT2 family. J Peripher Nerv Syst 2012;17:351–355.
4. Fu J, Dai S, Lu Y, et al. Similar clinical, pathological, and genetic features in Chinese patients with autosomal recessive and dominant Charcot-Marie-Tooth disease type 2K. Neuromuscul Disord 2017;27:760–765.
5. Zhang RX, Tang BS, Zi XH, et al. Mutation analysis of ganglioside-induced differentiation associated protein-1 gene in Chinese Charcot-Marie-Tooth disease. Zhonghua yi xue yi chuan xue za zhi = Zhonghua yixue yichuanxue zazhi = Chinese journal of medical genetics 2004;21:207–210.
6. Abe A, Numakura C, Kijima K, et al. Molecular diagnosis and clinical onset of Charcot-Marie-Tooth disease in Japan. J Hum Genet 2011;56:364–368.
7. Chung KW, Hyun YS, Lee HJ, et al. Two recessive intermediate Charcot-Marie-Tooth patients with GDAP1 mutations. J Peripher Nerv Syst 2011;16:143–146.
8. Lin KP, Soong BW, Yang CC, et al. The mutational spectrum in a cohort of Charcot-Marie-Tooth disease type 2 among the Han Chinese in Taiwan. PLoS One 2011;6: e29393.
9. Pakhrin PS, Xie Y, Hu Z, et al. Genotype-phenotype correlation and frequency of distribution in a cohort of Chinese Charcot-Marie-Tooth patients associated with GDAP1 mutations. J Neurol 2018;265:637–646.
10. Ben Othmane K, Hentati F, Lennon F, et al. Linkage of a locus (CMT4A) for autosomal recessive Charcot-Marie-Tooth disease to chromosome 8q. Hum Mol Genet 1993;2:1625–1628.
11. Baxter RV, Ben Othmane K, Rochelle JM, et al. Ganglioside-induced differentiation-associated protein-1 is mutant in Charcot-Marie-Tooth disease type 4A/8q21. Nat Genet 2002;30:21–22.
12. Cassereau J, Chevrollier A, Bonneau D, et al. A locus-specific database for mutations in GDAP1 allows analysis of genotype-phenotype correlations in Charcot-Marie-Tooth diseases type 4A and 2K. Orphanet J Rare Dis 2011;6:87.
13. Cassereau J, Chevrollier A, Gueguen N, et al. Mitochondrial dysfunction and pathophysiology of Charcot-Marie-Tooth disease involving GDAP1 mutations. Exp Neurol 2011;227:31–41.
14. Niemann A, Ruegg M, La Padula V, et al. Ganglioside-induced differentiation associated protein 1 is a regulator of the mitochondrial network: new implications for Charcot-Marie-Tooth disease. J Cell Biol 2005;170:1067–1078.
15. Pedrola L, Espert A, Valdes-Sanchez T, et al. Cell expression of GDAP1 in the nervous system and pathogenesis of Charcot-Marie-Tooth type 4A disease. J Cell Mol Med 2008;12:679–689.
16. Niemann A, Wagner KM, Ruegg M, Suter U. GDAP1 mutations differ in their effects on mitochondrial dynamics and apoptosis depending on the mode of inheritance. Neurobiol Dis 2009;36:509–520.
17. Lopez Del Amo V, Seco-Cervera M, Garcia-Gimenez JL, et al. Mitochondrial defects and neuromuscular degeneration caused by altered expression of Drosophila Gdap1: implications for the Charcot-Marie-Tooth neuropathy. Hum Mol Genet 2015;24:21–36.
18. Pla-Martin D, Rueda CB, Estela A, et al. Silencing of the Charcot-Marie-Tooth disease-associated gene GDAP1 induces abnormal mitochondrial distribution and affects Ca2+ homeostasis by reducing store-operated Ca2+ entry. Neurobiol Dis 2013;55:140–151.
19. Estela A, Pla-Martin D, Sanchez-Piris M, et al. Charcot-Marie-Tooth-related gene GDAP1 complements cell cycle delay at G2/M phase in Saccharomyces cerevisiae fis1 gene-defective cells. J Biol Chem 2011;286:36777–36786.
20. Fernandez-Lizarbe S, Civera-Tregon A, Cantarero L, et al. Neuroinflammation in the pathogenesis of axonal Charcot-Marie-Tooth disease caused by lack of GDAP1. Exp Neurol 2019;320:113004.
21. Li LX, Liu GL, Liu ZJ, et al. Identification and functional characterization of two missense mutations in NDRG1 associated with Charcot-Marie-Tooth disease type 4D. Hum Mutat 2017;38:1569–1578.
22. Chen CX, Dong HL, Wei Q, et al. Genetic spectrum and clinical profiles in a southeast Chinese cohort of Charcot-Marie-Tooth disease. Clin Genet 2019;96:439–448.
23. Yoshimura A, Yuan JH, Hashiguchi A, et al. Clinical and mutational spectrum of Japanese patients with Charcot-Marie-Tooth disease caused by GDAP1 variants. Clin Genet 2017;92:274–280.
24. Manganelli F, Tozza S, Pisciotta C, et al. Charcot-Marie-Tooth disease: frequency of genetic subtypes in a Southern Italy population. J Peripher Nerv Syst 2014;19:292–298.

25. Pezzini I, Geroldi A, Capponi S, et al. GDAP1 mutations in Italian axonal Charcot-Marie-Tooth patients: phenotypic features and clinical course. Neuromuscul Disord 2016;26:26–32.
26. Claramunt R, Pedrola L, Sevilla T, et al. Genetics of Charcot-Marie-Tooth disease type 4A: mutations, inheritance, phenotypic variability, and founder effect. J Med Genet 2005;42:358–365.
27. Zimon M, Battaloglu E, Parman Y, et al. Unraveling the genetic landscape of autosomal recessive Charcot-Marie-Tooth neuropathies using a homozygosity mapping approach. Neurogenetics 2015;16:33–42.
28. Sivera R, Sevilla T, Vilchez JJ, et al. Charcot-Marie-Tooth disease: genetic and clinical spectrum in a Spanish clinical series. Neurology 2013;81:1617–1625.
29. He J, Guo L, Xu G, et al. Clinical and genetic investigation in Chinese patients with demyelinating Charcot-Marie-Tooth disease. J Peripher Nerv Syst 2018;23:216–226.
30. Ammar N, Nelis E, Merlini L, et al. Identification of novel GDAP1 mutations causing autosomal recessive Charcot-Marie-Tooth disease. Neuromuscul Disord 2003;13:720–728.
31. Boerkoel CF, Takashima H, Nakagawa M, et al. CMT4A: identification of a Hispanic GDAP1 founder mutation. Ann Neurol 2003;53:400–405.
32. Parman Y, Battaloglu E, Baris I, et al. Clinicopathological and genetic study of early-onset demyelinating neuropathy. Brain 2004;127:2540–2550.
33. Georgiou DM, Nicolaou P, Chitayat D, et al. A novel GDAP1 mutation 439delA is associated with autosomal recessive CMT disease. Can J Neurol Sci 2006;33:311–316.
34. Noack R, Frede S, Albrecht P, et al. Charcot-Marie-Tooth disease CMT4A: GDAP1 increases cellular glutathione and the mitochondrial membrane potential. Hum Mol Genet 2012;21:150–162.
35. Huber N, Guimaraes S, Schrader M, et al. Charcot-Marie-Tooth disease-associated mutants of GDAP1 dissociate its roles in peroxisomal and mitochondrial fission. EMBO Rep 2013;14:545–552.
36. Cassereau J, Chevrollier A, Gueguen N, et al. Mitochondrial complex I deficiency in GDAP1-related autosomal dominant Charcot-Marie-Tooth disease (CMT2K). Neurogenetics 2009;10:145–150.
37. Huber N, Bieniossek C, Wagner K, et al. Glutathione-conjugating and membrane-remodeling activity of GDAP1 relies on amphipathic C-terminal domain. Sci Rep 2016;6:36930.
38. Legros F, Lombes A, Frachon P, Rojo M. Mitochondrial fusion in human cells is efficient, requires the inner membrane potential, and is mediated by mitofusins. Mol Biol Cell 2002;13:4343–4354.
39. Benard G, Bellance N, James D, et al. Mitochondrial bioenergetics and structural network organization. J Cell Sci 2007;120:838–848.

Supporting Information

Additional supporting information may be found online in the Supporting Information section at the end of the article.

Figure S1. Chromatograms of six known variants in two CMT-related genes were identified in the present study. The lower chromatogram in each frame represents the variant, while the upper one represents the normal sequence.

Figure S2. (A) Western blot analysis of protein extracts obtained from patient-derived fibroblasts of proband 2. The anti-GDAP1 antibody was used to detect the protein. (B) Values represent mean ± SD ($n = 3$, ****$P < 0.0001$). (C) MitoSOX Red staining was used to measure mitochondrial-specific ROS levels in fibroblasts from the Control and the patient. Hydrogen peroxide (H_2O_2) was used as the positive control. Scale bar, 1000 μm.

